Cell Reports
Physical Science

CellPress
OPEN ACCESS

Article

Topology as a limiting factor for mechanical properties in disordered networks

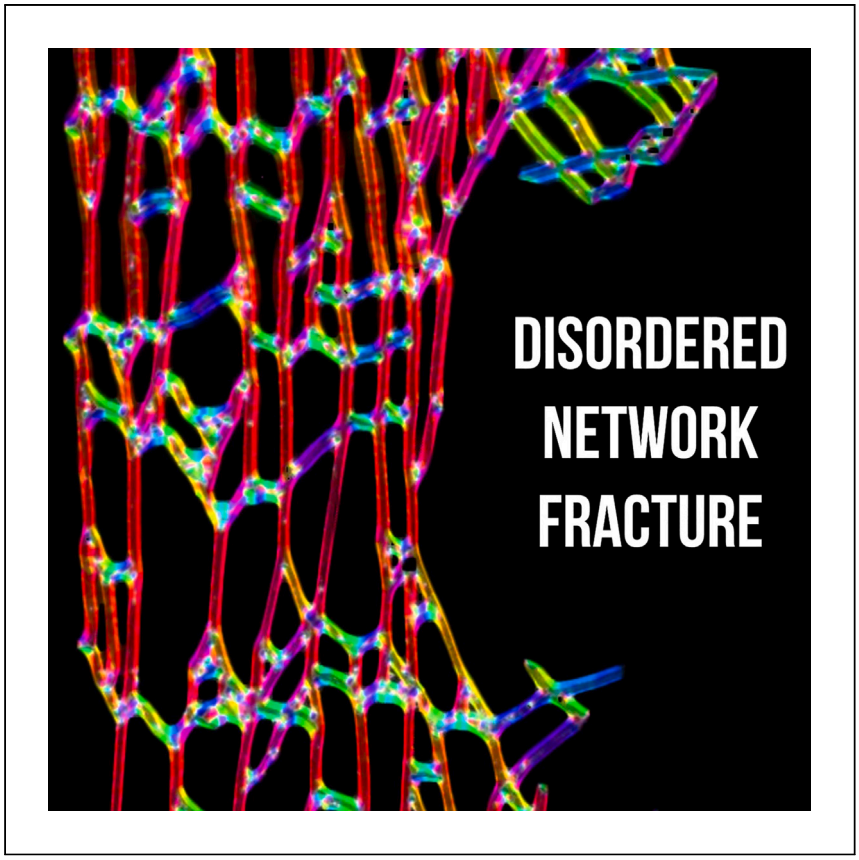

The beauty of nature lies in its ability to create materials with an extraordinary range of mechanical properties through the irregular arrangement of structural elements comprised of rather ordinary constituent materials. Drawing inspiration from these materials, Reyes-Martinez et al. show how architecture and intrinsic material properties can manipulate not only elastic response but also structural failure to design engineered materials with tailored mechanical behavior.

Marcos A. Reyes-Martinez, Edward J. Barron III, Dohgyu Hwang, Christopher L. Soles, Michael D. Bartlett, Edwin P. Chan

mbartlett@vt.edu (M.D.B.)
edwin.chan@nist.gov (E.P.C.)

Highlights

Constituent materials synergically combine with topology to tune mechanical properties

Work of fracture-network stiffness correlation can be reversed by material choice

A strategy to toughen networks on demand is demonstrated

Reyes-Martinez et al., Cell Reports Physical Science 5, 101848
March 20, 2024
https://doi.org/10.1016/j.xcrp.2024.101848

Please cite this article in press as: Reyes-Martinez et al., Topology as a limiting factor for mechanical properties in disordered networks, Cell Reports Physical Science (2024), https://doi.org/10.1016/j.xcrp.2024.101848

Cell Reports
Physical Science

Article

Topology as a limiting factor for mechanical properties in disordered networks

Marcos A. Reyes-Martinez,[1] Edward J. Barron III,[2,3] Dohgyu Hwang,[2,3] Christopher L. Soles,[1] Michael D. Bartlett,[2,3,4,*] and Edwin P. Chan[1,*]

SUMMARY

Disordered networks are ubiquitous in both natural and synthetic systems, with mechanical properties that span from significantly compliant to extremely rigid. While the significance of network topology in determining their overall mechanical properties has been established, the coupling between network topology and intrinsic material properties to control elasticity and fracture is not well understood. Here, we show that although the topology of two-dimensional disordered networks defines the occurrence of local network bond rupture events, it is the material properties of the constituent material that dictate the energy required to cause failure. Our results reveal opposite trends between the stiffness and fracture properties that depend on the constituent material, which is linked to how topology and materials couple to enhance either the local stiffness or extensibility of the network. We apply this understanding to transform the mechanical properties of an intrinsically low-toughness material to a tough one on demand.

INTRODUCTION

In nature, disordered networks are utilized to obtain materials with remarkable mechanical properties in diverse applications across a range of length scales.[1] These disordered networks consist of load-bearing elements, referred to here as "bonds," linked together at "nodes," forming aperiodic structures (Figure 1D). Depending on the ultimate purpose of the network, such as maximizing extensibility, load support, or toughness enhancement, there are important interactions between the geometry of load-bearing elements and the intrinsic properties of the constituent materials. For example, trabecular bone is a disordered network of bulky and rigid plates and struts where the composition and the network structure are optimized to support large loads and provide toughness while minimizing mass[6] (Figure 1A). Spiders, such as the orb-weaver tropical tent-web spider (cyrtophora citricola), also utilize disordered networks to create their webs. These slender, deformable filaments span across large interconnected areas that provide flexibility, toughness, and defect tolerance required to capture prey effectively (Figure 1B).[7] These biological examples illustrate the vast differences in length scale, material composition, and network connectivity, which give rise to extraordinary variation in ultimate mechanical properties. Importantly, these examples provide inspiration to design materials for diverse applications with tunable stiffness, toughness, and density by combining disordered network topology with different material properties.

Synthetic materials also utilize disordered networks, from large-scale support beams in some buildings (Figure 1C) to material-scale examples, including foams and

[1]National Institute of Standards and Technology (NIST), Materials Science and Engineering Division, Material Measurement Laboratory, Gaithersburg, MD 20899, USA

[2]Virginia Tech, Soft Materials and Structures Lab, Mechanical Engineering, Blacksburg, VA 24061, USA

[3]Virginia Tech, Macromolecules Innovation Institute, Blacksburg, VA 24061, USA

[4]Lead contact

*Correspondence: mbartlett@vt.edu (M.D.B.), edwin.chan@nist.gov (E.P.C.)

https://doi.org/10.1016/j.xcrp.2024.101848

Please cite this article in press as: Reyes-Martinez et al., Topology as a limiting factor for mechanical properties in disordered networks, Cell Reports Physical Science (2024), https://doi.org/10.1016/j.xcrp.2024.101848

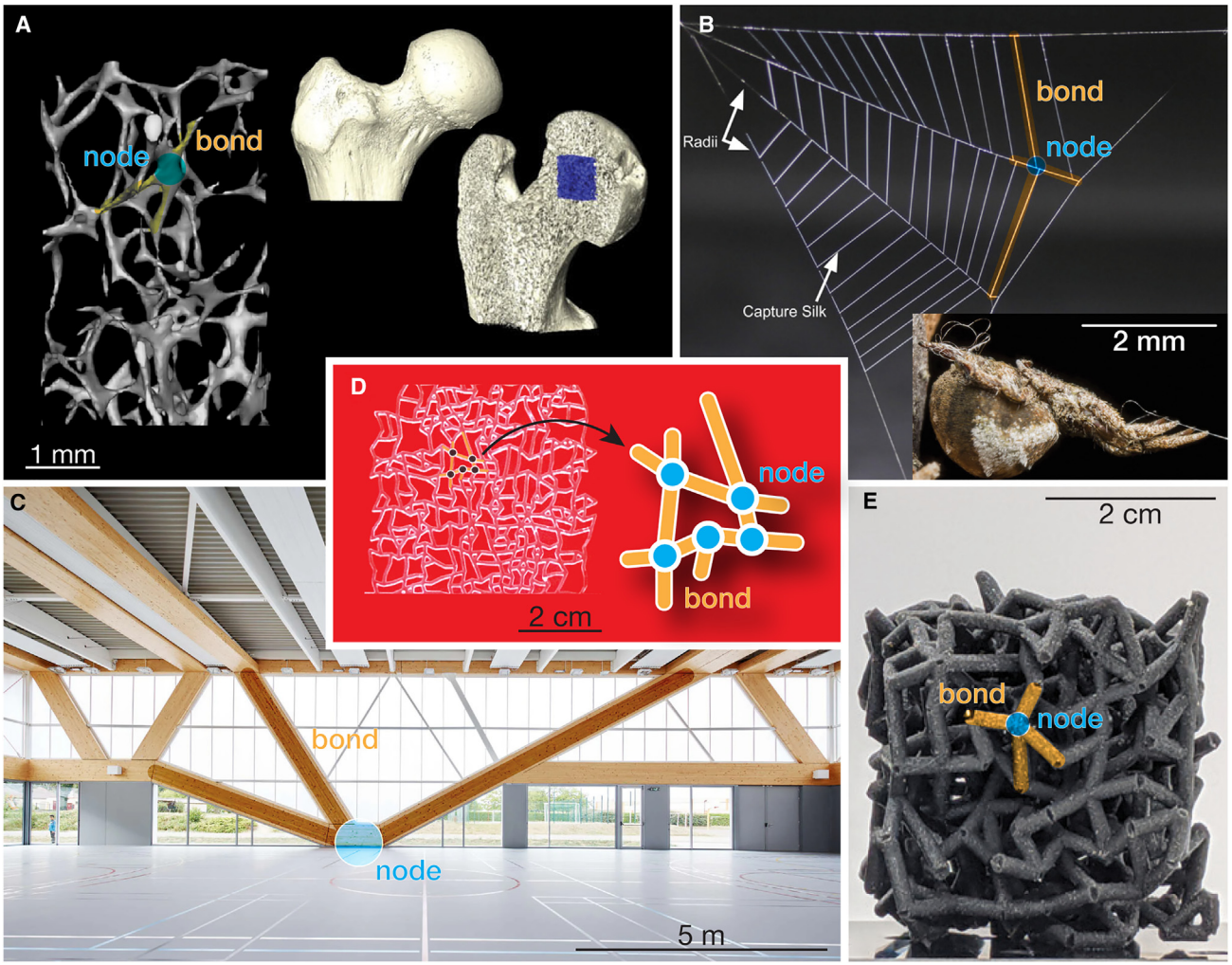

Figure 1. Examples of disordered networks found in nature and used in engineered structures

The fundamental unit for each structure consists of bonds linked by nodes that facilitate force and energy transmission.

(A) The structure of trabecular bone. Microcomputed tomography image of the internal structure of trabecular bone.[2] Reproduced with permission, Creative Commons 4.0. The two images correspond to trabecular bone. Reproduced with permission. 2019, American Journal of Physical Anthropology.[3]

(B) The structure of tent web built by the triangle weaver spider, *Hyptiotes cavatus*.[4] 2019, National Academy of Sciences, image by S.I. Han.

(C) The gallery of Nathalie Mauclair Gymnasium with support beams representing a human-made network structure. Reproduced with permission. 2015, David Foessel.

(D) A 2D disordered network made by laser cutting an acrylic sheet, which is the focus of this study. The fundamental structural unit consists of bonds connected by nodes.

(E) A representative 3D disordered network mechanical metamaterial made from 3D printing.[5] Reproduced with permission from the Royal Society of Chemistry.

honeycomb lattices.[8–10] Emerging approaches have enabled the generation of network-based materials through materials-by-design strategies. For example, computational approaches have demonstrated the design of disordered network mechanical metamaterials with tunable elastic properties by removing specific bonds[5,11–13](Figure 1E) or by optimizing the shape of bonds to improve the toughness of three-dimensional (3D) lattices.[14] Thermally programmable lattices, made of two polymers with different glass transition temperatures distributed at strategic topological locations within the network, have shown tunable global mechanical properties via different thermal conditions through local changes in mechanical

responses.[15] These developments illustrate the advantage of designing lightweight, strong, and responsive network materials based on the manipulation of local mechanical properties to obtain the desired global mechanical responses.

These biological and synthetic examples illustrate that properties such as global stiffness and toughness can potentially be manipulated in disordered networks. However, the specific means to control these mechanical properties through network topology and intrinsic material properties are not well understood. One important consideration is that architectured materials, such as disordered networks, are composed of discrete interconnected members. Thus, parameters from continuum mechanics may not be appropriate in characterizing their global elastic and fracture properties. For example, it has been shown by Deshpande and coworkers that the stress intensity factor, a parameter used to quantify the toughness of bulk materials, is inadequate when describing the fracture of ordered architectured materials because it can depend on system size, such as the geometry of the struts or the number of unit cells within the crack.[16–18]

An interesting characteristic of these disordered networks is that both the degree of disorder and member connectivity can independently control the brittle-to-ductile transition in network-based materials. Increasing the degree of disorder in a material decreases the stress concentration at the crack tip, thus facilitating a more diffuse fracture path.[19–21] Similarly, approaching the minimum bond connectivity to maintain topological rigidity, i.e., the rigidity percolation threshold, affects how a network fails by increasing the compliance of the system and the fracture process zone.[22,23] Although these prior studies demonstrated the importance of topology in defining this failure transition, how topology couples with the properties of the constituent material to control the overall mechanical properties of disordered-network-based materials is not well studied.

In this work, we demonstrate how topology, network density, and constituent material can be integrated to dictate the stiffness and fracture behavior of 2D disordered networks. We show results that are consistent with prior research; network topology controls the bond rupture events that are independent of the mechanical properties of the constituent material. However, we also demonstrate that topology alone does not completely dictate the mechanical properties of disordered network materials because the constituent material plays a critical role in controlling the deformation mechanism during failure. Specifically, the deformation mechanism transitions from bending dominated to stretching dominated as the constituent material softens, showing that the constituent material dictates the dominant mechanism of fracture, i.e., network stiffness vs. extensibility. Disordered networks with more compliant constituent materials show decreasing toughness with network stiffness, while stiffer constituent materials show increasing toughness with network stiffness. Based on these lessons, we suggest a practical route that enhances the work of fracture of disordered networks by tuning the intrinsic extensibility of a stiff constituent material. Our results demonstrate a design route based on the interplay between network topology, constituent stiffness, and extensibility for developing network-based materials with programmable stiffness and fracture properties.

RESULTS

2D disordered networks

We study the fracture behavior of disordered networks by fabricating physical samples of computationally conceived disordered networks (see the experimental

Please cite this article in press as: Reyes-Martinez et al., Topology as a limiting factor for mechanical properties in disordered networks, Cell Reports Physical Science (2024), https://doi.org/10.1016/j.xcrp.2024.101848

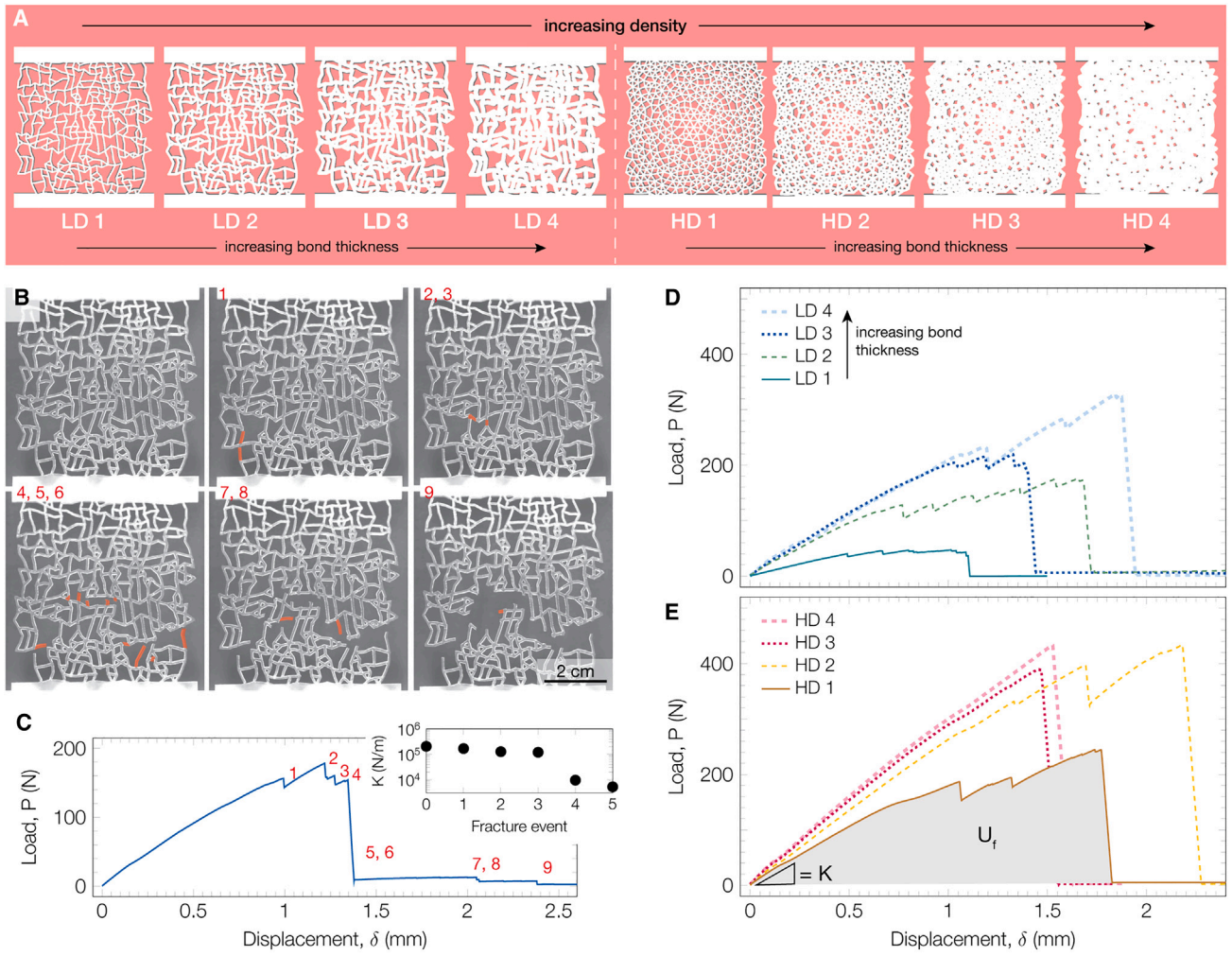

Figure 2. 2D disordered network geometries and results

(A) Structures of the 2D networks studied as a function of increasing mass density. Samples of both the low-density (LD) and high-density (HD) structures were produced with varying bond thicknesses: 0.5, 0.8, 1.2, and 1.6 mm, identified here with numbers 1–4.

(B) Photographs of representative tensile test on LD stiff network sample. Bonds that fail are highlighted in red.

(C) Instances of individual and collective bond failure are observed in the load-displacement curves in each tensile experiment. The inset shows the representative drop in stiffness as a function of the fracture event.

(D) Load-displacement curves corresponding to LD stiff networks with increasing bond thickness.

(E) Load-displacement curves corresponding to HD stiff networks with increasing bond thickness.

procedures). We use two base network structures corresponding to two different topologies, a low density (LD) with an average coordination number $Z = 3$ and a high density (HD) with an average coordination number $Z = 6$ (Figure 2A). The mass density and stiffness of each of these structures are then modified by varying the thickness of bonds = 0.5, 0.8, 1.2, and 1.6 mm, identified henceforth with numbers 1–4, respectively. Overall, samples from LD 1 to HD 4 make up a series of eight samples with various mass densities and topologies, as displayed in Figure 2A. The mass density of the HD samples is approximately 30%–65% larger than the LD counterparts of the same bond thickness. To understand the interplay between network topology and the intrinsic properties of the constituent material, we fabricate each network in Figure 2A using two materials: a stiff polymer (glassy acrylic) and a compliant polymer (rubbery silicone elastomer), both laser cut to the desired network structure.

Please cite this article in press as: Reyes-Martinez et al., Topology as a limiting factor for mechanical properties in disordered networks, Cell Reports Physical Science (2024), https://doi.org/10.1016/j.xcrp.2024.101848

Each of the physical network samples is subjected to uniaxial tension until complete failure is observed.

Figure 2B shows a representative uniaxial tension experiment of an LD 1 stiff network. At small displacements (δ<1 mm), the network deforms elastically, and no bonds are broken. At a critical tensile displacement, a bond or collection of bonds is broken. These broken bonds are highlighted in red, and the fracture events are enumerated in Figure 2B. At the moment of each bond rupture event, we see a sudden drop in load, as seen in the load-displacement curve in Figure 2C. After each bond rupture event, the tension is redistributed to the remaining bonds that are still connected to the network. The load builds back up until the next bond (or collection of bonds) ruptures. This behavior continues until the remaining bonds cannot support the load, and the structure fails catastrophically. After each bond rupture event, it can be seen that the load-displacement curve has a progressively lower slope, indicative of the whole structure progressively becoming more compliant as the number of load-bearing bonds decreases. The inset in Figure 2C quantifies this stiffness reduction as a function of fracture event.

Figures 2D and 2E show the load-displacement curves for representative families of stiff 2D disordered networks (LD and HD, respectively) for different bond thicknesses. We quantify the stiffness, K, for all network samples in the low extension regime (Figure 2E). The stiffness increases with the bond thickness for both the LD and HD samples. We also observe that the number of individual bond rupture events, represented by sudden drops in load in the load-displacement curves, decreases as the thickness of the bonds increases. This could be explained by the behavior of networks approaching the properties of a continuum as bond thickness, and therefore mass density, approaches that of the constituent material. Our results suggest that as bond thickness increases and bonds coalesce, the network becomes relatively more rigid, and the network tends to fail catastrophically as opposed to a stepwise manner.

Constituent material effects

Our study illustrates how coupling constituent materials with topology can enhance or diminish the elastic and fracture properties of architected materials. Figure 3A displays the load-displacement curves of representative LD 1 and HD 1 networks for both stiff and compliant constitutive materials. The compliant networks fail at displacements two orders of magnitude greater than the stiff networks. Interestingly, topology influences the fracture properties of the networks differently, depending on the constituent material being stiff or compliant. The compliant networks display similar maximum loads that are independent of the topology of the network. The stiff networks show remarkably different behavior, with the HD topology displaying higher maximum loads and failure displacements than the LD topology. This suggests that the contribution of network topology to the overall mechanical properties of the network greatly depends on the constituent material and is not universal. Insets in Figure 3A capture the extension and distortion of networks right before complete failure. Figure 3B shows the global stiffness, K, as a function of mass density, ρ, for LD and HD networks of compliant and stiff constituent materials. Consistent with classic studies on cellular solids, the network stiffness increases with the mass density of the network for each constituent material.[24] While the mass density is mainly dictated by the network topology and bond thickness, we observe that the network stiffness is dominated by the constituent material, with the stiff networks displaying K values that are nearly three orders of magnitude higher than the compliant ones.

Please cite this article in press as: Reyes-Martinez et al., Topology as a limiting factor for mechanical properties in disordered networks, Cell Reports Physical Science (2024), https://doi.org/10.1016/j.xcrp.2024.101848

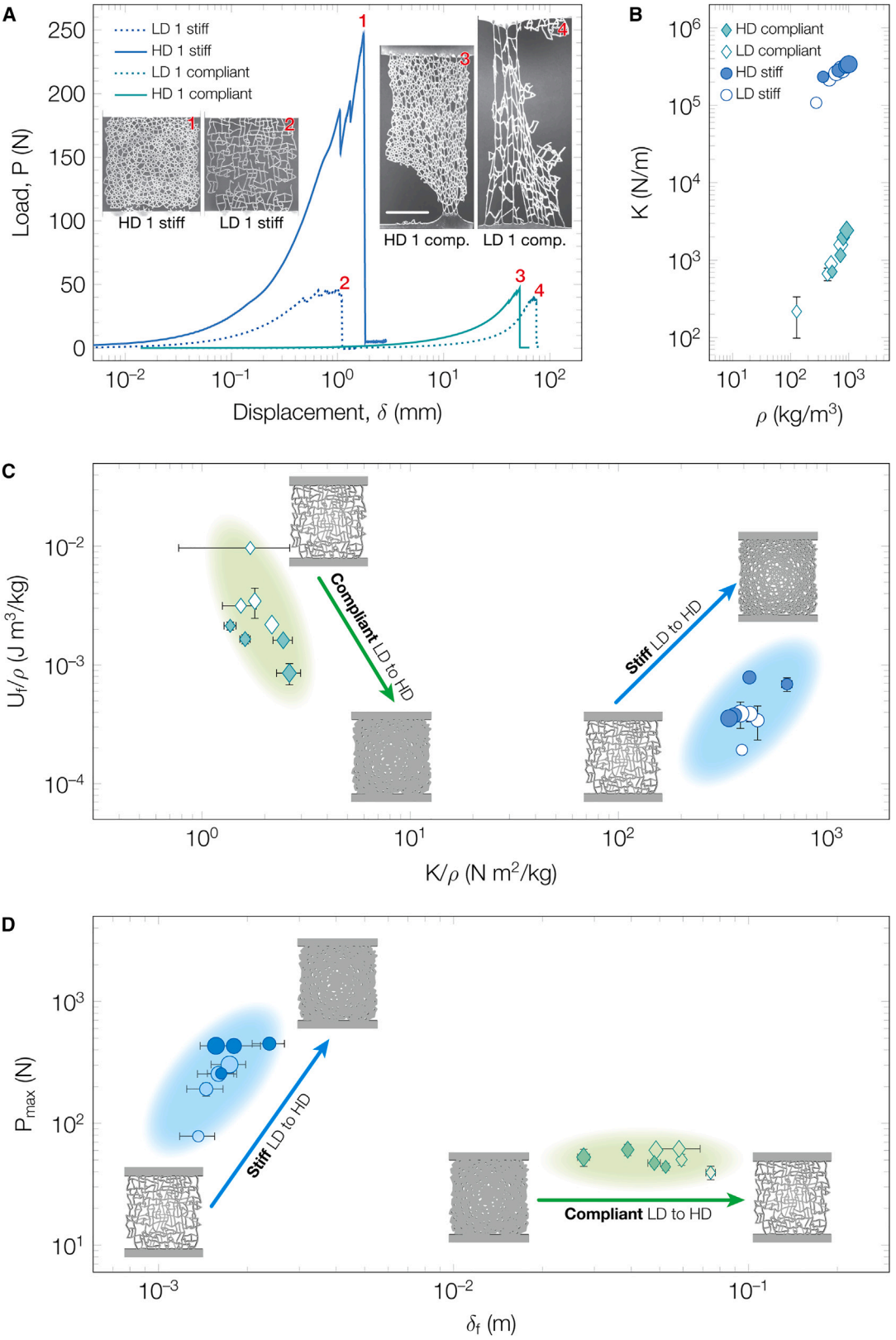

Please cite this article in press as: Reyes-Martinez et al., Topology as a limiting factor for mechanical properties in disordered networks, Cell Reports Physical Science (2024), https://doi.org/10.1016/j.xcrp.2024.101848

Figure 3. Elastic and fracture properties

(A) Load-displacement curves of representative LD 1 and HD 1 samples for both stiff and compliant constitutive materials. The curves suggest that topology is more significant in controlling the behavior of stiff networks compared to compliant networks. Insets capture the degree of extensibility right before complete failure. Scale bar = 2 cm.

(B) Network stiffness as a function of mass density of the sample. Mass density is mainly controlled by network topology and bond thickness, while stiffness depends on a combination of constituent material properties and network topology.

(C) Density-normalized work of fracture, U_f/ρ, as a function of density-normalized sample stiffness, K/ρ, for both stiff and compliant network samples. The work of fracture of the compliant network samples decreases as a function of stiffness, while the work of fracture for the stiff samples increases as a function of stiffness.

(D) Maximum load, P_{max}, as a function of fracture displacement, δ_f. The work of fracture of the stiff samples is dominated by P_{max}, while the compliant samples are dominated by δ_f. Increasing marker size represents increasing network bond thickness. Error bars represent the standard deviation over three independent experiments per network type.

To further show that the fracture behavior of disordered networks strongly depends on the constituent material, we quantify the work of fracture, U_f, by calculating the area under each load-displacement curve (Figure 2E). Figure 3C shows the density-normalized work of fracture (U_f/ρ) as a function of the density-normalized global network stiffness, K/ρ. Overall, our results show higher work of fracture for networks with compliant constituent material. Specifically, the highest U_f/ρ corresponds to the compliant LD networks with the thinnest bonds (i.e., inset 4, Figure 3A). Additionally, U_f/ρ decreases with increasing network stiffness for compliant samples. In contrast, the highest U_f/ρ for stiff networks corresponds to the HD networks, which are those with higher mass density and stiffness (i.e., inset 1, Figure 3A).

One of the defining characteristics differentiating the stiff and compliant networks is the extensibility of the constituent material. This difference is demonstrated in Figure 3D, which shows the maximum load, P_{max}, as a function of the failure displacement, δ_f, for all the networks studied. The compliant networks (both LD and HD) fail at larger displacements, given the hyperelastic nature of their constituent material (i.e., silicone elastomer), but display relatively low P_{max}. All of the compliant networks fail at displacements over an order of magnitude greater than the stiff networks. The large failure displacements and low maximum loads of compliant samples show that the work of fracture is primarily determined by the maximum extensibility. Conversely, the stiff networks display relatively high P_{max} values and low failure displacement, suggesting that the work of fracture is mainly dominated by the relatively high stiffness of the constituent material. As an example, the lowest mass density network (LD 1) displays the highest work of fracture for the compliant constituent material and the lowest work of fracture for the stiff constituent material (Figure 3C). Representative load-displacement curves for LD 1 networks are shown in Figure 3A. Given the topology of the LD network being less constrained ($Z = 3$), it is expected to promote extensibility and higher work of fracture. Nevertheless, that is not the case for the stiff networks, where the LD samples have both the lowest P_{max} and δ_f.

Bond orientation analysis

By tracking the changes in local deformation during our experiments, we observe that the different constituent materials undergo unique bond reorientation mechanisms as the network is deformed uniaxially. Figure 4A shows a compliant LD 1 network sample before tension is applied and immediately before the first bond rupture event is observed. The colors represent the angle of the bond relative to the direction of applied tension (here, 0° in light blue). At zero deformation, the bond angles show no preferred orientation. Upon deformation but before fracture, there is a clear preferential orientation along the direction of tension that is absent in the stiff samples (Figure 4B). Changes in bond orientations can be compared by

Please cite this article in press as: Reyes-Martinez et al., Topology as a limiting factor for mechanical properties in disordered networks, Cell Reports Physical Science (2024), https://doi.org/10.1016/j.xcrp.2024.101848

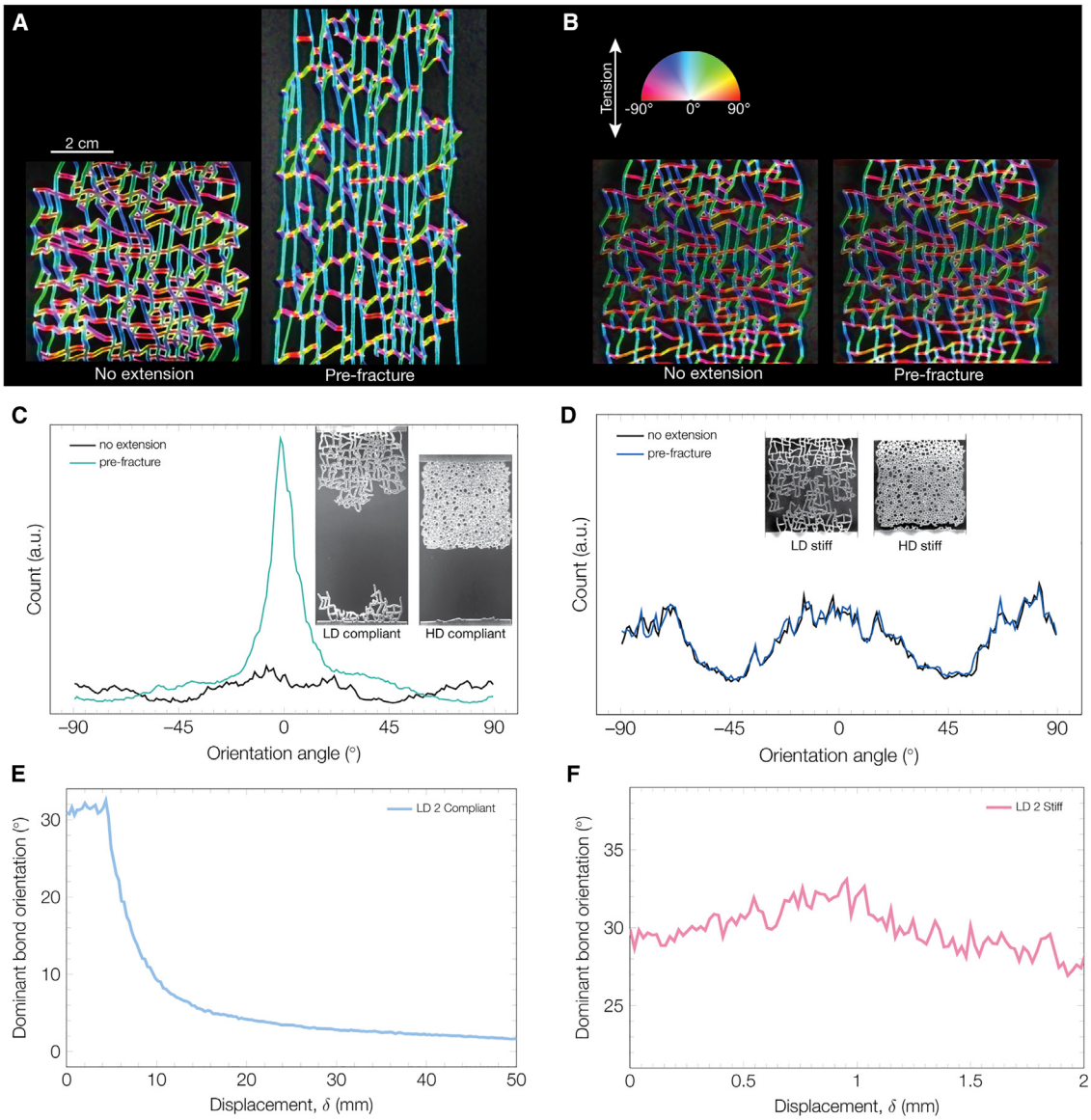

Figure 4. Bond orientation results of the undeformed and fractured disordered networks

(A and B) Bond orientation analysis for (A) LD 1 compliant and (B) LD 1 stiff samples. Colors indicate the bond orientation angle, as indicated in the legend.

(C and D) The corresponding histogram of the distribution of bond angles for (C) LD 1 compliant and (D) LD 1 stiff samples. The distribution of angles for the LD 1 stiff sample does not change before fracture, indicating that there is little or no change in bond orientation. Most of the bonds of the LD 1 compliant sample align along the tension direction (0°) right before the first fracture event occurs. The inset images compare the fractured portions of the HD and LD samples. Both the HD stiff and HD compliant samples display a straight crack near the edge of the sample. On the other hand, both the LD stiff and compliant samples show meandering cracks.

(E and F) The change in dominant bond orientation of representative (E) compliant network and (F) stiff networks as a function of applied displacement.

quantifying the distribution of bond angles of the representative compliant and stiff LD 1 networks. Figure 4C shows that the angle distribution changes drastically in the compliant sample, with a clear reorientation of bonds to the direction of tension, 0°. For the stiff LD 1 network, Figure 4D shows that the orientation distribution barely changes before and during applied tension, indicating very little bond reorientation up to the point of fracture. More detailed analyses of the bond orientation as a

Please cite this article in press as: Reyes-Martinez et al., Topology as a limiting factor for mechanical properties in disordered networks, Cell Reports Physical Science (2024), https://doi.org/10.1016/j.xcrp.2024.101848

function of deformation of representative compliant and stiff networks are shown in Figures 4E and 4F. The results, which confirm the trends observed in Figures 4C and 4D, show that the evolution of dominant bond orientation during the tensile experiment is strongly dependent on the particular constituent material. The initial bond orientation is the same for both networks, but the bond orientation deviates significantly with increasing displacement. Specifically, we find that the dominant bond orientation of the compliant network (Figure 4E) orients toward the tensile direction with increasing deformation, yet the stiff network (Figure 4F) displays only minor changes in the bond orientation. The magnitude of the work of fracture depends on the ability of the system to store strain energy before complete failure. On a local level, the development of strain energy can happen through bond stretching, bond bending, or combinations of both for 2D networks. The nearly imperceptible bond reorientation in the stiff samples indicates that these networks accommodate the buildup of strain energy by bending, rather than stretching, the bonds, which favors a stiffness-dominated work of fracture. However, for the compliant samples, the constituent material allows for early reorientation of the bonds and subsequent stretching, which favors an extensibility-dominated work of fracture.

The insets in Figures 4C and 4D show the fracture behavior for LD and HD networks for both constituent materials. Specifically, the HD networks undergo brittle failure, displaying a non-meandering distribution of bond fracture events. On the other hand, we find that the LD networks display a broad topological distribution of fractured bonds. These observations indicate that network topology, and not constituent material, plays a dominant role in the rupture of individual bonds. This is consistent with prior fracture studies of other disordered network systems.[22,23] We observe that for HD samples, individual bond fracture events tend to occur close to the grips; this behavior is not seen in the LD networks, which suggests that the HD network topology promotes stress concentration near the grips. Nevertheless, this particular phenomenon does not impact the conclusion that the distribution of locations of individual bond fracture events is controlled primarily by network topology and not the constituent material.

DISCUSSION

Our study shows that the intrinsic (constituent material) and extrinsic (topology) properties of disordered networks are intimately coupled to control the work of fracture, which is related to both the stiffness of the network and the maximum extension at fracture. Our results show (Figure 3D) that the work of fracture for stiff constituent materials is primarily controlled by bond bending, which translates to significantly higher failure loads compared to the compliant samples. For compliant constituent materials, the work of fracture is dominated by the stretching and rearrangement of the bonds, which translates to higher maximum extensions at failure. This insight is consistent with the trends in our tensile experiments; the disordered networks with softer constituent materials show decreasing work of fracture with network stiffness, while stiffer constituent materials show increasing work of fracture with network stiffness (Figure 3C). This interplay between topology design and material selection results in the highest work of fracture corresponding to compliant materials with the lowest mass density networks. These networks show significant stretching not only due to the innate extensibility of the constituent material but also due to the low bond connectivity that can accommodate isolated bond rupture events without catastrophic failure. Importantly, Figure 3C shows that the trend in the work of fracture can be reversed by the judicious choice of the constituent material. The use of a compliant constituent material renders the network more tolerant to

Please cite this article in press as: Reyes-Martinez et al., Topology as a limiting factor for mechanical properties in disordered networks, Cell Reports Physical Science (2024), https://doi.org/10.1016/j.xcrp.2024.101848

inhomogeneities in stress distribution, resulting in higher work of fracture for the lowest density networks. Networks comprised of stiff constituent material are less tolerant to stress inhomogeneities, and therefore the higher work of fracture corresponds to denser network architectures.

Our tensile experiments show that fracture can be controlled either by the stiffness or extensibility of the material. Determining whether stiffness or extensibility should be enhanced requires an appreciation of the mechanical behavior of the intrinsic material. This lesson has inspired the design of numerous different tough materials in the past, such as particle-reinforced composites,[25–27] double-network hydrogels,[28–31] macroscale double networks,[32,33] and topoarchitected polymer networks.[34] However, these prior approaches rely primarily on multi-component materials, whereby each component is dedicated to a specific function. Taking the macroscale double network as an example, the brittle network provides enhanced stiffness, whereas the soft one provides extensibility. Here, we are interested in enhancing the toughness of a single-component material.

As a proof of concept, we demonstrate this single-component control using temperature as a stimulus to enhance the stiffness or extensibility of disordered networks composed of poly(methyl methacrylate) (PMMA) as the constituent material. Similar to other viscoelastic polymers, PMMA is stiff (glassy) but brittle at room temperature, yet it is compliant (rubbery) and highly extensible at elevated temperatures. We conducted temperature-conditioned uniaxial tensile experiments on four different network systems (LD 1, LD 4, HD 1, and HD 4) to assess their fracture behavior. Figure 5A is a schematic showing the procedure of the temperature-conditioned tension experiments. In stage 1 of the experiment, each network is stretched at room temperature to the pre-fracture displacement, which maximizes the stiffness-dominated behavior of PMMA. In stage 2, the sample is heated to 140°C while the displacement is held constant. This portion of the test is intended to soften the PMMA to leverage network extensibility for toughness enhancement. Once the sample has thermally equilibrated, tension is applied again until failure. The thermal (Figure 5B) and bright-field (Figure 5C) images of the stretched networks show that this thermal-conditioning process can stretch PMMA well beyond what is possible at room temperature, which we envision is broadly applicable to other materials with a thermal transition. Figure 5D shows the work of fracture, U_f, for all samples tested as a function of network structure. The highest U_f corresponds to the thermally conditioned HD 1 network, which was shown in Figure 3 to be dominated by the stiffness of the constitutive material at room temperature. Depending on the specific network, Figure 5D shows that the work of fracture of the disordered networks subjected to this temperature conditioning process can be enhanced by as much as two orders of magnitude. Figure 5E shows the normalized work of fracture $\overline{U}_f = U_{f,therm}/U_{f,0}$ as a function network stiffness, where $U_{f,therm}$ refers to the work of fracture of the thermally conditioned networks and $U_{f,0}$ is the work of fracture of the same networks at room temperature. These results show that lower stiffness networks show greater $\overline{U}_f$. This trend is consistent with the behavior observed in Figure 3C for the compliant networks, where more compliant networks show greater work of fracture. This points to the importance of underlying material properties controlling fracture properties in disordered network systems. It is interesting to note that in Figure 3C, the enhancement is achieved by reducing the density of the network by either reducing the bond thickness or changing the topology. In Figure 5E, the work of fracture enhancement obtained via thermal conditioning does not require changing the constituent material or substituting it with a different network topology.

Please cite this article in press as: Reyes-Martinez et al., Topology as a limiting factor for mechanical properties in disordered networks, Cell Reports Physical Science (2024), https://doi.org/10.1016/j.xcrp.2024.101848

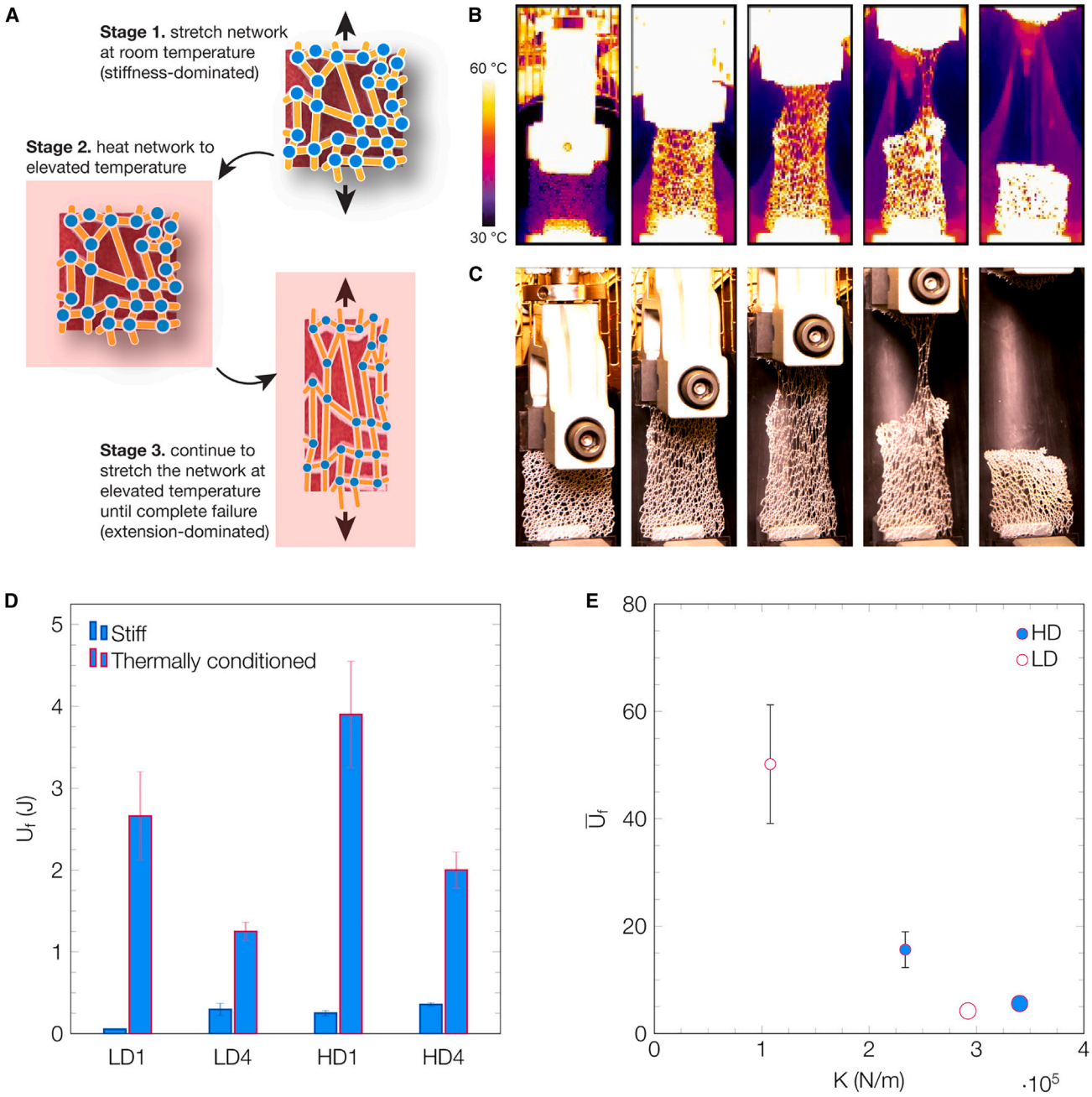

Figure 5. Tuning the stiffness and extensibility of brittle disordered networks via thermal conditioning

(A) Experimental procedure of the thermal-conditioned tension experiments. In stage 1, the network is stretched at room temperature to the pre-fracture displacement, which maximizes the stiffness-dominated behavior of PMMA. In stage 2, the network is heated to 140°C while the extension is kept constant. This portion of the test is intended to soften the PMMA to maximize network extensibility for toughness enhancement. In stage 3, the network has equilibrated to the elevated temperature, and tension is further applied until the network has completely failed.

(B and C) Thermal (B) and bright-field (C) images of a representative network undergoing the thermal-conditioned tension experiment showing that the PMMA is able to stretch well beyond what is possible at room temperature.

(D) Work of fracture (U_f) as a function network topology. Stiff samples LD 1, LD 4, HD 1, and HD 4 are thermally treated at 140°C. An increase of two orders of magnitude in the work of fracture is observed for the heated stiff (acrylic) samples stretched at a displacement rate of 1 mm/s. Error bars represent the standard deviation over three independent experiments per network type.

(E) Normalized work of fracture $\overline{U}_f = U_{f,\mathrm{therm}}/U_{f,0}$ as a function network stiffness, where $U_{f,\mathrm{therm}}$ refers to the work of fracture of the thermally conditioned networks and $U_{f,0}$ is the work of fracture of the same networks at room temperature.

By leveraging the bond-to-bond variation in the load-bearing capacity of a disordered network, we show that it is possible to dynamically manipulate the stiffness and extensibility of the individual material elements. As local regions of a disordered network experience non-uniform stress and strain distributions, these networks enable a greater degree of programmability in local mechanical response. The results in Figure 5B show that depending on the local bond density of the network, the denser regions experience a greater temperature rise, thus leading to greater extensibility during stage 3. Although this thermal-conditioning approach is a simple demonstration, these results illustrate the potential to program the mechanical properties of mechanical metamaterials via the synergistic combination of a viscoelastic polymer and disordered network topology. Such capabilities could also be combined into ordered networks, heterogeneous networks, and other multi-component systems to tune mechanical properties and function.[35–37] With the appropriate selection of intrinsic material and network topology, other stimuli, such as light, solvent exposure, electric, and magnetic fields, can be used to manipulate the local mechanical properties of these disordered networks.

In this study, we show that the coupling between constituent materials and topology can either enhance or diminish the elastic and fracture properties of architected materials. Importantly, we demonstrated that topology alone does not completely dictate the mechanical properties of disordered network materials; it is the synergy between architecture, materials, and function that ultimately defines the mechanical properties of these network materials. Thus, it is important to develop quantitative relationships between topology and materials further in future studies, although this is a non-trivial endeavor. Our proposed thermal conditioning of bonds illustrates one pragmatic strategy to program mechanical behavior that overcomes the intrinsic limits of materials via a combination of geometry, strain localization, and programmable extensibility without the need for multiple constituent materials. There are several opportunities (different stimuli, length scale of load-bearing elements, and dynamics of stress transfer) to leverage this concept to overcome the intrinsic limitations of existing materials and to design mechanically programmable materials.

EXPERIMENTAL PROCEDURES

Resource availability

Lead contact

Further information and requests for resources should be directed to and will be fulfilled by the lead contact, Michael D. Bartlett (mbartlett@vt.edu).

Materials availability

This study did not generate new unique reagents.

Data and code availability

The data that support the findings of this study are available from the corresponding authors upon reasonable request.

2D disordered network mechanical metamaterial fabrication

Drawings of LD and HD 2D disordered networks are based on random packing of jammed frictionless spheres obtained from previous work by Reid et al.[12] The computational realizations used are of isotactic networks of equal-stiffness springs. These drawings are then integrated into a dog-bone-like design amenable to tensile testing. The length and width of the network samples are held constant for all

samples at 60 × 56 mm, respectively. Four bond thicknesses of LD and HD structures are produced: 0.5, 0.8, 1.2, and 1.6 mm.

Stiff network samples are fabricated by laser cutting (Full Spectrum Laser) 1.5 ± 0.1 mm thick Plexiglass sheets (McMaster-Carr). Compliant network samples are also fabricated by laser cutting 1.6 ± 0.1 mm thick poly(dimethylsiloxane) (PDMS) elastomer sheets (Sylgard 184 with a 10:1 base-to-curing agent mass ratio; Dow Corning) created by curing PDMS pre-polymers within an acrylic mold. Compliant network samples were meticulously cleaned after laser cutting to remove any dry residue from the cutting process.

Mechanical testing

Room temperature tensile tests were performed using a Texture Analyzer TA.XT Plus instrument using custom-made grips and a 50 kg load cell. Stiff samples were tested at a rate of 0.1 mm/s, while compliant samples were tested at 1 mm/s. The displacement is reported from instrument cross-head readout. Tension was applied until the samples failed completely. At least three individual experiments were performed for each sample type. Images of experiments were captured using a charge-coupled device camera (JAI BM500GE) operating at 30 fps. Orientation analysis of images was performed using ImageJ OrientationJ plugin.[38]

Tensile tests at elevated temperatures were performed using an Instron 5900 series Universal Testing System (Instron: 5969) with a 50 kN load cell and an Instron 3119 series Environmental Chamber (Instron: 3119-609) for heating. Stiff samples LD 1, LD 4, HD 1 and HD 4 were first stretched at room temperature at a rate of 0.05 mm/s to a pre-fracture displacement of 2 mm, which is prior to the first fracture event of the materials. The samples are then held at constant displacement for 15 min as the environmental chamber is heated to 140°C. Once the sample temperature was equilibrated, tension was applied to the thermally conditioned specimens at a rate of 1 mm/s until the samples failed completely. At least three individual experiments were performed for each sample.

Images were captured through a separate testing procedure. HD 1 samples were stretched at room temperature at a rate of 0.05 mm/s until 2 mm of displacement. Images of the sample were captured with both a digital single-lens reflex (DSLR) camera (Pentax K-1 Mark II) and an infrared (IR) thermal imaging camera (FLIR E53). The sample was heated to 140°C for 15 min prior to being stretched to a displacement of 30 mm at a rate of 1 mm/s. The environmental chambers were opened, and images were captured using the DSLR and IR cameras. The environmental chamber was then closed, and the process was repeated at displacement intervals of 30 mm until complete sample failure.

ACKNOWLEDGMENTS

E.J.B., D.H., and M.D.B. acknowledge support from Virginia Tech and the Office of Naval Research Young Investigator Program (YIP) (N000142112699). M.A.R.-M. and E.P.C. acknowledge Dr. Daniel R. Reid and Dr. Nidhi Pashine (University of Chicago) for providing the design of the network structures used in this study. Certain instruments, software, and materials are identified in this work to adequately specify the experimental details. Such identification does not imply a recommendation by the National Institute of Standards and Technology, nor does it imply that the materials are necessarily the best available for the purpose.

AUTHOR CONTRIBUTIONS

M.A.R.-M., M.D.B., and E.P.C. conceived, designed, and analyzed room temperature fracture experiments. M.A.R.-M. performed room temperature fracture experiments. E.J.B. performed thermal conditioning fracture experiments and associated analysis. D.H. fabricated elastomeric network samples. M.A.R.-M., M.D.B., and E.P.C. wrote the first and final versions of the manuscript. All authors discussed the experiments and gave consent for this publication under the supervision of M.D.B. and E.P.C.

DECLARATION OF INTERESTS

The authors declare no competing interests.

Received: July 11, 2023
Revised: January 17, 2024
Accepted: February 5, 2024
Published: March 5, 2024

REFERENCES

1. Metzler, R.A., Barthelat, F., and Wilker, J.J. (2019). Disordered structures in biology can provide material properties not obtained with precise hierarchy. Adv. Funct. Mater. *29*, 1805734. https://doi.org/10.1002/adfm.201805734.

2. Glantschnig, H., Hampton, R.A., Lu, P., Zhao, J.Z., Vitelli, S., Huang, L., Haytko, P., Cusick, T., Ireland, C., Jarantow, S.W., et al. (2010). Generation and selection of novel fully human monoclonal antibodies that neutralize Dickkopf-1 (DKK1) inhibitory function in vitro and increase bone mass in vivo. J. Biol. Chem. *285*, 40135–40147. https://doi.org/10.1074/jbc.M110.166892.

3. Doershuk, L.J., Saers, J.P.P., Shaw, C.N., Jashashvili, T., Carlson, K.J., Stock, J.T., and Ryan, T.M. (2019). Complex variation of trabecular bone structure in the proximal humerus and femur of five modern human populations. Am. J. Phys. Anthropol. *168*, 104–118. https://doi.org/10.1002/ajpa.23725.

4. Han, S.I., Astley, H.C., Maksuta, D.D., and Blackledge, T.A. (2019). External power amplification drives prey capture in a spider web. Proc. Natl. Acad. Sci. USA *116*, 12060–12065. https://doi.org/10.1073/pnas.1821419116.

5. Reyes-Martinez, M.A., Chan, E.P., Soles, C.L., Han, E., Murphy, K.A., Jaeger, H.M., Reid, D.R., and de Pablo, J.J. (2022). Tuning the mechanical impedance of disordered networks for impact mitigation. Soft Matter *18*, 2039–2045. https://doi.org/10.1039/d1sm01649k.

6. Oftadeh, R., Perez-Viloria, M., Villa-Camacho, J.C., Vaziri, A., and Nazarian, A. (2015). Biomechanics and mechanobiology of trabecular bone: A review. J. Biomech. Eng. *137*, 010802. https://doi.org/10.1115/1.4029176.

7. Su, I., Qin, Z., Saraceno, T., Krell, A., Mühlethaler, R., Bisshop, A., and Buehler, M.J. (2018). Imaging and analysis of a three-dimensional spider web architecture. J. R. Soc. Interface *15*, 20180193. https://doi.org/10.1098/rsif.2018.0193.

8. Gibson, L.J. (1981). The Elastic and Plastic Behaviour of Cellular Materials. Ph.D. thesis (University of Cambridge).

9. Gibson, L.J., and Ashby, M.F. (1982). The mechanics of three-dimensional cellular materials. Proc. Math. Phys. Eng. Sci. *382*, 43–59. https://doi.org/10.1098/rspa.1982.0088.

10. Ashby, M.F. (2006). The properties of foams and lattices. Philos. Trans. R. Soc. A *364*, 15–30. https://doi.org/10.1098/rsta.2005.1678.

11. Goodrich, C.P., Liu, A.J., and Nagel, S.R. (2015). The principle of independent bond-level response: Tuning by pruning to exploit disorder for global behavior. Phys. Rev. Lett. *114*, 225501. https://doi.org/10.1103/PhysRevLett.114.225501.

12. Reid, D.R., Pashine, N., Wozniak, J.M., Jaeger, H.M., Liu, A.J., Nagel, S.R., and de Pablo, J.J. (2018). Auxetic metamaterials from disordered networks. Proc. Natl. Acad. Sci. USA *115*, E1384–E1390. https://doi.org/10.1073/pnas.1717442115.

13. Hexner, D., Liu, A.J., and Nagel, S.R. (2018). Role of local response in manipulating the elastic properties of disordered solids by bond removal. Soft Matter *14*, 312–318. https://doi.org/10.1039/c7sm01727h.

14. Lee, S., Zhang, Z., and Gu, G.X. (2022). Generative machine learning algorithm for lattice structures with superior mechanical properties. Mater. Horiz. *9*, 952–960. https://doi.org/10.1039/d1mh01792f.

15. Mueller, J., Lewis, J.A., and Bertoldi, K. (2022). Architected multimaterial lattices with thermally programmable mechanical response. Adv. Funct. Mater. *32*, 2105128. https://doi.org/10.1002/adfm.202105128.

16. O'Masta, M., Dong, L., St-Pierre, L., Wadley, H., and Deshpande, V. (2017). The fracture toughness of octet-truss lattices. J. Mech. Phys. Solids *98*, 271–289. https://doi.org/10.1016/j.jmps.2016.09.009.

17. Shaikeea, A.J.D., Cui, H., O'Masta, M., Zheng, X.R., and Deshpande, V.S. (2022). The toughness of mechanical metamaterials. Nat. Mater. *21*, 297–304. https://doi.org/10.1038/s41563-021-01182-1.

18. Indurkar, P.P., Shaikeea, A., Xu, Z., Cui, H., Zheng, X., and Deshpande, V. (2022). The coupled strength and toughness of interconnected and interpenetrating multi-material gyroids. MRS Bull. *47*, 461–473. https://doi.org/10.1557/s43577-021-00249-3.

19. Roux, S., Hansen, A., Herrmann, H., and Guyon, E. (1988). Rupture of heterogeneous media in the limit of infinite disorder. J. Stat. Phys. *52*, 237–244. https://doi.org/10.1007/bf01016411.

20. Curtin, W.A., and Scher, H. (1990). Brittle fracture in disordered materials: A spring network model. J. Mater. Res. *5*, 535–553. https://doi.org/10.1557/JMR.1990.0535.

21. Shekhawat, A., Zapperi, S., and Sethna, J.P. (2013). From damage percolation to crack nucleation through finite size criticality. Phys. Rev. Lett. *110*, 185505. https://doi.org/10.1103/PhysRevLett.110.185505.

22. Driscoll, M.M., Chen, B.G.-g., Beuman, T.H., Ulrich, S., Nagel, S.R., and Vitelli, V. (2016). The role of rigidity in controlling material failure. Proc. Natl. Acad. Sci. USA *113*, 10813–10817. https://doi.org/10.1073/pnas.1501169113.

23. Berthier, E., Kollmer, J.E., Henkes, S.E., Liu, K., Schwarz, J.M., and Daniels, K.E. (2019). Rigidity percolation control of the brittle-ductile transition in disordered networks. Phys. Rev. Mater. *3*, 075602. https://doi.org/10.1103/PhysRevMaterials.3.075602.

24. Gibson, L.J., and Ashby, M.F. (1997). Cellular Solids: Structure and Properties. Cambridge Solid State Science Series (Cambridge University Press).

25. Ahmed, S., and Jones, F.R. (1990). A review of particulate reinforcement theories for polymer

composites. J. Mater. Sci. *25*, 4933–4942. https://doi.org/10.1007/bf00580110.

26. Kim, B.C., Park, S.W., and Lee, D.G. (2008). Fracture toughness of the nano-particle reinforced epoxy composite. Compos. Struct. *86*, 69–77. https://doi.org/10.1016/j.compstruct.2008.03.005.

27. Lauke, B. (2008). On the effect of particle size on fracture toughness of polymer composites. Compos. Sci. Technol. *68*, 3365–3372. https://doi.org/10.1016/j.compscitech.2008.09.011.

28. Gong, J., Katsuyama, Y., Kurokawa, T., and Osada, Y. (2003). Double-network hydrogels with extremely high mechanical strength. Adv. Mater. *15*, 1155–1158. https://doi.org/10.1002/adma.200304907.

29. Gong, J.P. (2010). Why are double network hydrogels so tough? Soft Matter *6*, 2583–2590. https://doi.org/10.1039/b924290b.

30. Chen, Q., Chen, H., Zhu, L., and Zheng, J. (2015). Fundamentals of double network hydrogels. J. Mater. Chem. B *3*, 3654–3676. https://doi.org/10.1039/c5tb00123d.

31. Zhang, W., Liu, X., Wang, J., Tang, J., Hu, J., Lu, T., and Suo, Z. (2018). Fatigue of double-network hydrogels. Eng. Fract. Mech. *187*, 74–93. https://doi.org/10.1016/j.engfracmech.2017.10.018.

32. King, D.R., Okumura, T., Takahashi, R., Kurokawa, T., and Gong, J.P. (2019). Macroscale double networks: Design criteria for optimizing strength and toughness. ACS Appl. Mater. Interfaces *11*, 35343–35353. https://doi.org/10.1021/acsami.9b12935.

33. King, D.R. (2022). Macroscale double networks: highly dissipative soft composites. Polym. J. *54*, 943–955. https://doi.org/10.1038/s41428-022-00646-8.

34. Liu, X., Wu, J., Qiao, K., Liu, G., Wang, Z., Lu, T., Suo, Z., and Hu, J. (2022). Topoarchitected polymer networks expand the space of material properties. Nat. Commun. *13*, 1622. https://doi.org/10.1038/s41467-022-29245-0.

35. Shu, X., Mao, Y., Lei, M., Da, D., Hou, S., and Zhang, P. (2022). Toughness enhancement of honeycomb lattice structures through heterogeneous design. Mater. Des. *217*, 110604. https://doi.org/10.1016/j.matdes.2022.110604.

36. Hwang, D., Barron, E.J., III, Haque, A.B.M.T., and Bartlett, M.D. (2022). Shape morphing mechanical metamaterials through reversible plasticity. Sci. Robot. *7*, eabg2171. https://doi.org/10.1126/scirobotics.abg2171.

37. Wang, S., Hu, Y., Kouznetsova, T.B., Sapir, L., Chen, D., Herzog-Arbeitman, A., Johnson, J.A., Rubinstein, M., and Craig, S.L. (2023). Facile mechanochemical cycloreversion of polymer cross-linkers enhances tear resistance. Science *380*, 1248–1252. https://doi.org/10.1126/science.adg3229.

38. Püspöki, Z., Storath, M., Sage, D., and Unser, M. (2016). Transforms and operators for directional bioimage analysis: A survey. In Focus on Bio-Image Informatics (Springer International Publishing), pp. 69–93.